Feshbach spectroscopy of an ultracold mixture of ^{85}Rb and ^{133}Cs

Hung-Wen Cho,[1] Daniel J. McCarron,[1] Michael P. Köppinger,[1] Daniel L. Jenkin,[1] Kirsteen L. Butler,[1] Paul S. Julienne,[2] Caroline L. Blackley,[3] C. Ruth Le Sueur,[3] Jeremy M. Hutson,[3] and Simon L. Cornish[1]

[1]*Joint Quantum Centre (JQC) Durham/Newcastle, Department of Physics, Durham University, Durham DH1 3LE, United Kingdom*
[2]*Joint Quantum Institute, NIST and the University of Maryland, Gaithersburg, Maryland 20899-8423, USA*
[3]*Joint Quantum Centre (JQC) Durham/Newcastle, Department of Chemistry, Durham University, Durham DH1 3LE, United Kingdom*
(Received 9 August 2012; published 11 January 2013)

We report the observation of interspecies Feshbach resonances in an optically trapped mixture of ^{85}Rb and ^{133}Cs. We measure nine resonances in the lowest spin channel for a magnetic field range from 0 to 700 G and show that they are in good agreement with coupled-channel calculations. The interspecies background scattering length is close to zero over a large range of magnetic fields, permitting the sensitive detection of Feshbach resonances through interspecies thermalization. Our results confirm the quality of the Rb-Cs potential curves [Phys. Rev. A **85**, 032506 (2012)] and offer promising starting points for the production of ultracold polar molecules.

Ultracold polar molecules provide numerous new and exciting avenues of research for studies of dilute quantum systems [1,2]. The permanent electric dipole moments possessed by these molecules give rise to anisotropic, long-range dipole-dipole interactions which are in contrast to the isotropic, short-range interactions commonly encountered in ultracold atomic gas experiments [3]. These dipole-dipole interactions can operate over a range greater than typical optical lattice separations leading to a range of novel quantum phases and opportunities for quantum simulation and quantum information processing [4–6].

The most promising route toward realizing these proposals exploits a two-step indirect method where the constituent atoms in a mixed-species quantum gas are associated into ground-state molecules [7]. Weakly bound molecules are first made by magnetoassociation using a Feshbach resonance [8] and are then optically transferred into the rovibrational ground state by stimulated Raman adiabatic passage (STIRAP) [9]. Great strides have been made using this approach in a number of systems [10–12], although the only polar molecule that has so far been produced at high phase-space density is fermionic KRb [10]. However, two KRb molecules can undergo an exothermic reaction to form $K_2 + Rb_2$ [13]. An attractive alternative is to form ground-state RbCs, which is expected to be collisionally stable because both the exchange reaction $2RbCs \rightarrow Rb_2 + Cs_2$ and trimer formation reactions are endothermic [14]. There has been considerable work on the Feshbach resonances [15] and molecule formation [16,17] in ^{87}Rb^{133}Cs. However, this isotopologue has an interspecies background scattering length that is large and positive, which produces a spatial separation of the dual condensate [18] and enhances losses from three-body collisions [19,20]. Both of these factors inhibit the formation of weakly bound Feshbach molecules.

In this paper, we explore the alternative mixture of ^{85}Rb and ^{133}Cs, which we show does not suffer from the problems present for the mixture of ^{87}Rb and ^{133}Cs. We report the observation of nine interspecies Feshbach resonances, which are all in excellent agreement with coupled-channel calculations. We show that the interspecies background scattering length is close to zero over a large range of magnetic fields,

permitting the sensitive detection of Feshbach resonances through interspecies thermalization. Our observations, together with detailed calculations of the near-threshold bound-state spectrum, reveal numerous possible gateways into the realm of ultracold heteronuclear molecules.

Details of our apparatus have been described previously in the context of our work on dual-species condensates of ^{87}Rb and ^{133}Cs [18,19]. Ultracold mixtures of ^{85}Rb and ^{133}Cs are collected in a two-species magneto-optical trap. The ^{85}Rb and ^{133}Cs atoms are optically pumped into the $|2, -2\rangle$ and $|3, -3\rangle$ states, respectively, and then loaded into a magnetic quadrupole trap. Forced rf evaporation cools the ^{85}Rb atoms to 50 μK while ^{133}Cs is cooled sympathetically by interspecies elastic collisions. Further efficient evaporative cooling is inhibited by Majorana losses [21]. The two species are then transferred into a crossed dipole trap formed using the output of a single-frequency 30 W, 1550 nm fiber laser. After loading, the ^{85}Rb and ^{133}Cs atoms are transferred into the $|2, +2\rangle$ and $|3, +3\rangle$ states, respectively, by rf adiabatic rapid passage [22], and a vertical magnetic field gradient of 21.2 G/cm is applied, just below the 22.4 G/cm required to levitate ^{85}Rb [23]. The resulting gravitational sag of the ^{133}Cs cloud ($\lesssim 2$ μm) is significantly less than the typical vertical full width at half-maximum (FWHM) of the cloud ($\simeq 24$ μm), so that there is excellent spatial overlap of both species throughout the measurement. The magnetic field gradient also results in a field spread of $\simeq 0.05$ G across the cloud, which limits the minimum observed resonance width. The magnetic field is calibrated using microwave spectroscopy between the hyperfine states of ^{133}Cs.

A typical experiment starts with a mixture of $2.0(1) \times 10^5$ ^{85}Rb atoms at 7.9(1) μK and $2.3(1) \times 10^4$ ^{133}Cs atoms at 10.6(5) μK confined in the dipole trap in the lowest spin channels. The temperature difference between the two species arises from a combination of the small interspecies background scattering length and the differing trap depths for the two species: at 1550 nm, the polarizability of ^{133}Cs is ~ 1.4 times greater than that of ^{85}Rb. The significant atom number imbalance between the two species increases the sensitivity of heteronuclear Feshbach spectroscopy. Here the ^{133}Cs atoms act as a probe species immersed in a collisional bath of

^{85}Rb [24]. To perform Feshbach spectroscopy, the magnetic field is switched to a specific value in the range 0–700 G. Evaporative cooling is then performed by reducing the laser power by a factor of 4 over 2 s to final trap depths of 15 μK for ^{85}Rb and 22 μK for ^{133}Cs. The mixture is then held for 1 s in this final trapping potential. To probe the mixture, resonant absorption images of both species are captured in each experimental cycle using a frame-transfer CCD camera. Interspecies Feshbach resonances are identified by studying the variation in the atom number and temperature for both species with magnetic field.

The rich Feshbach resonance structure of this system is shown in Fig. 1. The top panel shows a coarse scan of the ^{85}Rb (●) and ^{133}Cs (○) temperatures between 0 and 700 G. Each point corresponds to an average of at least three repeated measurements. The bottom panel shows the scattering length and the energies of the near-threshold molecular states, obtained from coupled-channel calculations as described below. Over a large range of magnetic field, the magnitude of the interspecies scattering length is <60 bohr (indicated by the gray shaded region) and the two species do not equilibrate to a common temperature within the duration of the experiment. However, the variation of the scattering length in the vicinity of an interspecies resonance produces a pronounced feature in the ^{133}Cs temperature as the ^{133}Cs atoms are sympathetically cooled by the colder ^{85}Rb atoms. The large windows of thermal equilibrium around 110 and 640 G coincide with broad s-wave resonances. Additionally, many narrow resonances

can be identified in very good agreement with the calculated Feshbach spectrum. The positions of experimental resonances are marked by arrows whose positions are determined by fine scans across each resonance. Solid arrows mark s-wave features while dashed arrows mark two observed p-wave resonances.

The two dotted arrows in Fig. 1 mark features induced by the dipole trapping lasers. The two laser beams that form the optical trap are offset in frequency from one another by 100 MHz in order to prevent the formation of an optical lattice. The two features at 233.9(2) and 246.5(3) G are observed when one beam is polarized parallel to the magnetic field direction and the other is perpendicular to it. They are strongly suppressed when both beams are polarized either parallel or perpendicular to the magnetic field direction, but can be recovered by applying a 100 MHz rf magnetic field perpendicular to the local quantization field. This suggests that the laser-induced features in Fig. 1 arise from a two-photon Raman coupling to bound or quasibound states of the ^{85}RbCs molecule with $M_F = +4$ or $+6$.

Figure 2 shows an example of a fine scan across the interspecies resonance at 187.66(5) G. Here the thermalization between the two species on resonance is clear as ^{133}Cs is sympathetically cooled by ^{85}Rb [Fig. 2(a)]. The sympathetic cooling also enhances the ^{133}Cs number remaining in the trap while the additional heat load on ^{85}Rb leads to further evaporative trap loss [Fig. 2(b)]. The lines correspond to Lorentzian fits to the data. In general, the experimental
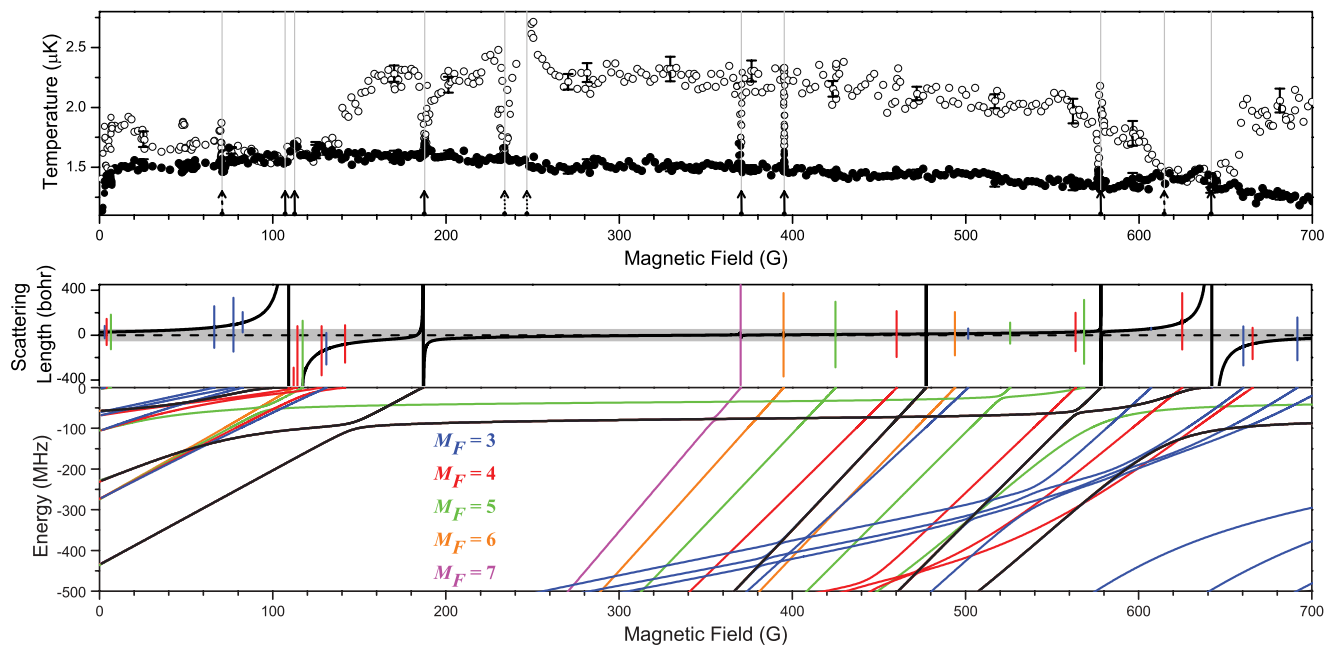

FIG. 1. (Color online) Top: Observation of interspecies Feshbach resonances by thermalization of the two species for fields up to 700 G. The closed (open) symbols indicate the ^{85}Rb (^{133}Cs) temperature while solid (dashed) arrows mark observed s-wave (p-wave) resonances and dotted arrows mark laser-induced features. Error bars show the standard deviations for multiple control shots at specific magnetic fields. Bottom: The calculated s-wave interspecies scattering length and weakly bound molecular states for the same field range. Bound states arising from $L = 0$ (s states) are shown as black lines while those from $L = 2$ (d states) are shown in other colors that indicate the value of M_F (see figure). The bound-state energies are plotted relative to the energy of the lowest hyperfine state of ^{85}Rb + ^{133}Cs, the $|2, +2\rangle + |3, +3\rangle$ hyperfine level. Resonance positions are marked on the scattering length plot using vertical lines of the same color as the corresponding bound state; the length of each line is proportional to the logarithm of the width of the resonance. The gray shaded region indicates where $|a| < 60$ bohr. All the bound states shown are for $M_{tot} = 5$, corresponding to s-wave scattering in the lowest channel.
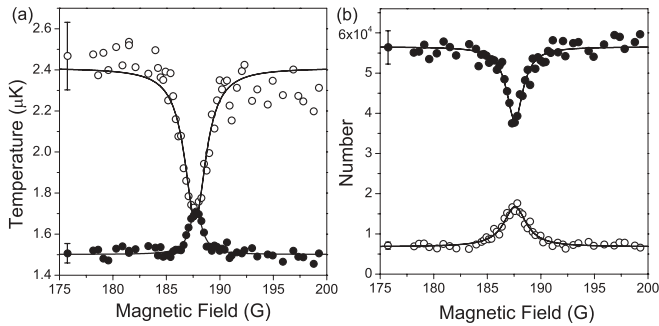
FIG. 2. An interspecies resonance observed at 187.66(5) G. The closed (open) symbols indicate ^{85}Rb (^{133}Cs) data points. (a) Temperature data for both species reveal the thermalization of ^{133}Cs with ^{85}Rb at and near the resonance highlighting the tunable nature of the sympathetic cooling. (b) Atom number data show the ^{133}Cs number to increase while the ^{85}Rb number decreases when a resonance is crossed and sympathetic cooling occurs. Error bars show the standard deviation for multiple control shots at a specific magnetic field.

positions (B_0) and widths (δ) of the resonances are determined from weighted averages of the fits to the four features illustrated in Fig. 2. However, in some cases fewer than four fits are possible because only the number or temperature results show pronounced features: for example, only the number results show pronounced features in the broad window of thermal equilibrium near 110 G.

Intra- and interspecies Feshbach resonances are distinguished as shown in Fig. 3. In this region, the ^{85}Rb number shows two loss features [Fig. 3(a)]. The resonance at 368.78(3) G results in no change of the ^{133}Cs temperature, indicating that this feature is an ^{85}Rb intraspecies resonance [Fig. 3(b)]. Conversely, near the feature at 370.39(1) G, the two species come into thermal equilibrium through sympathetic cooling, showing this to be an interspecies resonance. This interpretation is confirmed by performing single-species measurements. Further details on the observed ^{85}Rb intraspecies resonances will be presented in Ref. [25].
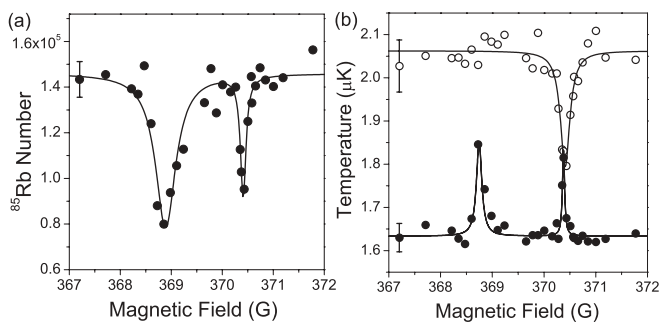

FIG. 3. An intraspecies ^{85}Rb resonance at 368.78(3) G neighboring an interspecies resonance at 370.39(1) G. Closed (open) symbols indicate ^{85}Rb (^{133}Cs) data. (a) Loss of ^{85}Rb reveals both resonances. (b) Temperature data allow the resonances to be distinguished as intra- or interspecies. The ^{133}Cs temperature is unchanged at the ^{85}Rb intraspecies resonance but decreases at the interspecies resonance at higher field where interspecies collisions cause sympathetic cooling. Error bars show the standard deviation for multiple control shots at a specific magnetic field.

The interspecies scattering length and bound-state positions are calculated from a coupled-channel model, using the potential curves of Ref. [17], which were fitted to Fourier transform spectra of both ^{85}Rb^{133}Cs and ^{87}Rb^{133}Cs and Feshbach resonances and weakly bound states of ^{87}Rb^{133}Cs. All the calculations are carried out in a fully uncoupled basis set, $|s_{Rb}m_{sRb}\rangle |i_{Rb}m_{iRb}\rangle |s_{Cs}m_{sCs}\rangle |i_{Cs}m_{iCs}\rangle |LM_L\rangle$, where s and i indicate electron and nuclear spins and L is the quantum number for end-over-end rotation of the two atoms about one another. The coupled equations are diagonal in the total projection quantum number $M_{tot} = M_L + M_F$, where $M_F = m_{sRb} + m_{iRb} + m_{sCs} + m_{iCs}$. The basis sets used here include all functions with $L = 0$ and 2 for incoming $L = 0$ (s-wave) and with $L = 1$ and 3 for incoming $L = 1$ (p-wave).

The scattering calculations are carried out using the MOLSCAT program [26], as modified to handle collisions in an external field [27]. The calculations use a fixed-step log-derivative propagator [28] to propagate from 0.3 to 1.9 nm and then the variable-step Airy propagator [29] to propagate from 1.9 to 1500 nm. The s-wave scattering length is obtained from $a(k) = (ik)^{-1}(1 - S_{00})/(1 + S_{00})$ [30], where S_{00} is the diagonal S-matrix element in the incoming channel and k is the corresponding wave vector. For incoming $L = 1$, a and k are replaced by a^3 and k^3. Single-channel calculations on the singlet and triplet potential curves of Ref. [17] give singlet and triplet scattering lengths of 585.6 and 11.27 bohr, respectively.

The bound-state calculations use the associated packages BOUND [31] and FIELD, which locate bound states by solving sets of coupled differential equations in the same basis set as for scattering calculations, as described for alkali-metal dimers in Ref. [32]. BOUND locates the energies of bound states at fixed magnetic field, whereas FIELD locates the magnetic fields at which bound states exist at fixed binding energy.

In the vicinity of a resonance, the scattering length is given approximately by $a(B) = a_{bg}\{1 - [\Delta/(B - B_0)]\}$. The width Δ is thus conveniently calculated for each resonance as $B_* - B_0$, where B_* is the field where $a(B)$ crosses zero and B_0 is the location of the corresponding pole. The MOLSCAT package is capable of converging directly on both these points. However, it should be noted that theoretical widths defined in this way are not the same thing as the fitted experimental Lorentzian widths δ, and the two should not be compared.

The experimental and theoretical resonance parameters are compared in Table I. Most of the experimentally observed resonance positions are in good agreement with the theoretical predictions [33]. The success of mass scaling between ^{87}Rb^{133}Cs and ^{85}Rb^{133}Cs demonstrates the accuracy of the potential curves, and in particular confirms that they support the correct absolute number of bound states. This agreement extends over features measured for both incoming s- and p-wave collisions [34].

Our observations show that the interspecies background scattering length is close to zero over a large range of magnetic fields. This reduces losses due to interspecies three-body collisions for ^{85}Rb + ^{133}Cs and makes it much easier to achieve good overlap of atomic clouds than for ^{87}Rb + ^{133}Cs. The broad resonances near 110 and 640 G will permit precise tuning of the interatomic interactions, allowing control of the miscibility and studies of Efimov physics in heteronuclear

TABLE I. Feshbach resonances for ^{85}Rb $|2, +2\rangle + {}^{133}$Cs $|3, +3\rangle$ in the field range 0–700 G. All resonances with calculated widths $\Delta > 0.01$ G are listed. See the supplemental material for a complete listing of the s-wave resonances, including narrower ones [35]. The experimental errors in B_0 and δ are statistical uncertainties resulting from the fits as described in the text. Additional systematic uncertainties of 0.1 and 0.5 G apply to the experimental resonance positions in the field ranges 0–400 and 400–700 G, respectively.

Experiment		Theory							
B_0	δ	Assignment				B_0	B_*	Δ	a_{bg}
(G)	(G)	L_i	L	F	M_F	(G)	(G)	(G)	(bohr)
70.68(4)	0.8(1)	p	1			70.54	58.54	−12	
		s	2	4	3	77.51	77.52	0.010	93.6
107.13(1)	0.6(2)	s	0	5	5	109	350	241	9.6
112.6(4)	28(5)	s	2	6	6	112.29	112.12	−0.17	−628
		s	2	4	4	114.33	114.21	−0.12	−246
		s	2	6	5	117.40	117.35	−0.051	−169
187.66(5)	1.7(3)	s	0	6	5	187.07	182.97	−4.1	−30.3
370.39(1)	0.08(4)	s	2	7	7	370.41	374.31	3.9	1.57
395.20(1)	0.08(1)	s	2	7	6	395.11	395.56	0.45	3.4
		s	2	7	5	425.11	425.16	0.045	6.1
		s	2	5	5	568.62	568.66	0.037	29.8
577.8(1)	1.1(3)	s	0	6	5	578.36	578.7 0	0.34	32.2
614.6(3)	1.1(4)	p	1			614.98	608.18	−6.8	
		s	2	5	4	625.29	625.30	0.014	123
641.8(3)	6(2)	s	0	5	5	642	901	259	9.6
		s	2	3	3	708.70	708.68	−0.024	−23.8

systems. There are also numerous narrower resonances with widths in the range that is convenient for magnetoassociation. Future work will include exploration of the molecular bound states (Fig. 1) by magnetic-field modulation spectroscopy, magnetoassociation to form weakly bound molecules, and optical transfer to the ground state. ^{85}Rb^{133}Cs offers the prospect of forming a gas of ultracold polar molecules that are stable with respect to chemical reactions.

[1] L. D. Carr, D. DeMille, R. V. Krems, and J. Ye, New J. Phys. **11**, 055049 (2009).

[2] B. Friedrich and J. M. Doyle, ChemPhysChem **10**, 604 (2009).

[3] T. Lahaye, C. Menotti, L. Santos, M. Lewenstein, and T. Pfau, Rep. Prog. Phys. **72**, 126401 (2009).

[4] B. Capogrosso-Sansone, C. Trefzger, M. Lewenstein, P. Zoller, and G. Pupillo, Phys. Rev. Lett. **104**, 125301 (2010).

[5] A. Micheli, G. Pupillo, H. P. Büchler, and P. Zoller, Phys. Rev. A **76**, 043604 (2007).

[6] M. L. Wall and L. D. Carr, New J. Phys. **11**, 055027 (2009).

[7] B. Damski, L. Santos, E. Tiemann, M. Lewenstein, S. Kotochigova, P. Julienne, and P. Zoller, Phys. Rev. Lett. **90**, 110401 (2003).

[8] C. Chin, R. Grimm, E. Tiesinga, and P. S. Julienne, Rev. Mod. Phys. **82**, 1225 (2010).

[9] K. Bergmann, H. Theuer, and B. W. Shore, Rev. Mod. Phys. **70**, 1003 (1998).

[10] K.-K. Ni, S. Ospelkaus, M. H. G. de Miranda, A. Pe'er, B. Neyenhuis, J. J. Zirbel, S. Kotochigova, P. S. Julienne, D. S. Jin, and J. Ye, Science **322**, 231 (2008).

[11] F. Lang, K. Winkler, C. Strauss, R. Grimm, and J. Hecker Denschlag, Phys. Rev. Lett. **101**, 133005 (2008).

[12] J. G. Danzl, M. J. Mark, E. Haller, M. Gustavsson, R. Hart, J. Aldegunde, J. M. Hutson, and H.-C. Nägerl, Nat. Phys. **6**, 265 (2010).

[13] S. Ospelkaus, K.-K. Ni, D. Wang, M. H. G. de Miranda, B. Neyenhuis, G. Quéméner, P. S. Julienne, J. L. Bohn, D. S. Jin, and J. Ye, Science **327**, 853 (2010).

[14] P. S. Żuchowski and J. M. Hutson, Phys. Rev. A **81**, 060703 (2010).

[15] K. Pilch, A. D. Lange, A. Prantner, G. Kerner, F. Ferlaino, H.-C. Nägerl, and R. Grimm, Phys. Rev. A **79**, 042718 (2009).

[16] M. Debatin, T. Takekoshi, R. Rameshan, L. Reichsöllner, F. Ferlaino, R. Grimm, R. Vexiau, N. Bouloufa, O. Dulieu, and H.-C. Nägerl, Phys. Chem. Chem. Phys. **13**, 18926 (2011).

[17] T. Takekoshi, M. Debatin, R. Rameshan, F. Ferlaino, R. Grimm, H.-C. Nägerl, C. R. Le Sueur, J. M. Hutson, P. S. Julienne, S. Kotochigova, and E. Tiemann, Phys. Rev. A **85**, 032506 (2012).

[18] D. J. McCarron, H. W. Cho, D. L. Jenkin, M. P. Köppinger, and S. L. Cornish, Phys. Rev. A **84**, 011603 (2011).

[19] H. W. Cho, D. J. McCarron, D. L. Jenkin, M. P. Köppinger, and S. L. Cornish, Eur. Phys. J. D **65**, 125 (2011).

[20] A. D. Lercher, T. Takekoshi, M. Debatin, B. Schuster, R. Rameshan, F. Ferlaino, R. Grimm, and H.-C. Nägerl, Eur. Phys. J. D **65**, 3 (2011).

[21] Y.-J. Lin, A. R. Perry, R. L. Compton, I. B. Spielman, and J. V. Porto, Phys. Rev. A **79**, 063631 (2009).

[22] D. L. Jenkin, D. J. McCarron, M. P. Köppinger, H. W. Cho, S. A. Hopkins, and S. L. Cornish, Eur. Phys. J. D **65**, 11 (2011).

[23] Units of Gauss rather than Tesla, the accepted SI unit for the magnetic field, have been used in this paper to conform to the conventional usage in this field of physics.

[24] E. Wille, F. M. Spiegelhalder, G. Kerner, D. Naik, A. Trenkwalder, G. Hendl, F. Schreck, R. Grimm, T. G. Tiecke, J. T. M. Walraven, S. J. J. M. F. Kokkelmans, E. Tiesinga, and P. S. Julienne, Phys. Rev. Lett. **100**, 053201 (2008).

[25] C. L. Blackley, C. R. Le Sueur, J. M. Hutson, D. J. McCarron, M. P. Köppinger, H. W. Cho, D. L. Jenkin, and S. L. Cornish, arXiv:1212.5446.

[26] J. M. Hutson and S. Green, *MOLSCAT Computer Program, Version 14* (CCP6, Daresbury, 1994).

[27] M. L. González-Martínez and J. M. Hutson, Phys. Rev. A **75**, 022702 (2007).

[28] D. E. Manolopoulos, J. Chem. Phys. **85**, 6425 (1986).

[29] M. H. Alexander, J. Chem. Phys. **81**, 4510 (1984).

[30] J. M. Hutson, New J. Phys. **9**, 152 (2007).

[31] J. M. Hutson, *BOUND Computer Program, Version 5* (CCP6, Daresbury, 1993).

[32] J. M. Hutson, E. Tiesinga, and P. S. Julienne, Phys. Rev. A **78**, 052703 (2008).

[33] Comparison between theory and experiment for the cluster of resonances near 110 G is limited by the fact that not all resonances are resolved experimentally.

[34] The two *p*-wave resonances that are observed experimentally have calculated widths >6 G, and all others have calculated widths < 0.3 G.

[35] See Supplemental Material at http://link.aps.org/supplemental/10.1103/PhysRevA.87.010703 for a complete listing of the *s*-wave resonances, including narrower ones.